Minimal energy packings of nearly flexible polymers

Robert S. Hoy[1],[*] Jared Harwayne-Gidansky[2,5], and Corey S. O'Hern[3,4,5]
[1] *Department of Physics, University of South Florida, Tampa, FL 33620 and*
Departments of Electrical Engineering[2]*, Mechanical Engineering & Materials Science*[3]*, Physics*[4]*,*
and [5]*Integrated Graduate Program in Physical and Engineering Biology, Yale University, New Haven, CT*
(Dated: October 16, 2012)

We extend recent studies of the minimal energy packings of short flexible polymers with hard-core-like repulsions and short-range attractions to include bond-angle interactions with the aim of describing the collapsed conformations of 'colloidal' polymers. We find that flexible tangent sticky-hard-sphere (t-SHS) packings provide a useful perturbative basis for analyzing polymer packings with nonzero bending stiffness only for *small* ratios of the stiffnesses for the bond-angle and pair interactions, $k_b^{\rm crit}/k_c \lesssim 0.01$ for $N < 10$, and the critical ratio decreases with the number of monomers N. Thus we argue that future studies should not use flexible t-SHS minimal energy packings as a reference set to enumerate and characterize the structural and mechanical properties of polymer packings with finite bending stiffness.

PACS numbers: 64.70.km,81.16.Dn,02.10.Ox,87.15.hp

arXiv:1210.3712v1 [cond-mat.soft] 13 Oct 2012

Protein folding and other examples of polymer collapse in dilute solutions are complex processes that involve the cooperative motion of thousands of atoms. A number of early studies of polymer and protein structure and dynamics employed hard-sphere models with only steric interactions, bond-length, and bond-angle constraints to understand polymer elasticity[1] as well as secondary structure[2] and packing in hydrophobic cavities[3] in proteins. More recent studies have implemented Monte Carlo, Brownian dynamics, and molecular dynamics (MD) simulations that include excluded volume and stereochemical constraints as well as solvent-mediated attractive interactions to investigate numerous examples of polymer collapse. However, recent advances in colloidal synthesis and self assembly have enabled studies of "colloidal polymers" with hard-core-like repulsions, short-range attractions, and greater chain flexibility than typical synthetic or biological polymers[4, 5], which has prompted renewed interest in simple polymer models. We seek to develop the ability to theoretically predict which structures are most likely to form for a given set of interactions and solvent conditions, which will reduce the need for trial-and-error synthesis of self-assembled nanostructures.

The ground state packings of short, flexible tangent sticky hard sphere (t-SHS) polymers have recently been characterized via complete enumeration techniques.[6] These packings possess a wider range of symmetries and shapes than the ground state packings of polymers with longer-ranged attractive (*e.g.* Lennard-Jones[7]) pair potentials. Further, the number $N_{\rm micro}$ of distinguishable, energetically degenerate ground-state flexible t-SHS packings ("microstates") grows exponentially with the polymerization index N, with a corresponding increase in the diversity of paths followed by the covalent backbones. In this manuscript, we will characterize the ground state packings for short, *semi-flexible* t-SHS polymers with finite bending stiffness k_b using the ground-state flexible t-SHS polymer packings as a reference set. In particular, we will calculate the potential energy of semi-flexible polymer packings as a function of k_b and identify the maximum bending stiffness $k_b^{\rm crit}$ below which the reference set of t-SHS packings are the lowest energy structures. These studies will inform future exact-enumeration studies of polymer packings with larger bending stiffness.

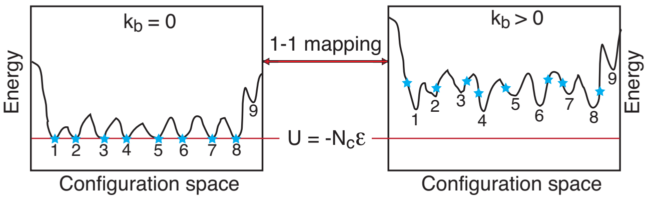

FIG. 1: Schematic of the low-lying minima in the energy landscape for polymer packings as a function of the configurational degrees of freedom $\{\vec{r}\}$. For vanishing bending stiffness $k_b = 0$ (left), the ground-state flexible polymer packings (stars) are energetically degenerate and correspond to the lowest $N_{\rm micro}$ inherent structures (minima of the black curve). Increasing k_b (right) deforms the energy landscape and raises the energies of the $N_{\rm micro}$ minima that correspond to the flexible polymer packings. For $k_b < k_b^{\rm crit}$, the $N_{\rm micro}$ lowest energy semi-flexible polymer packings correspond to the $N_{\rm micro}$ ground-state flexible polymer packings.

Figure 1 summarizes our theoretical approach. Consider a polymer model with harmonic pair and bond-angle potentials with respective "spring constants" k_c and k_b, and equilibrium bond angle θ_{eq}. The ground-state flexible ($k_b = 0$) t-SHS polymer packings can provide a useful reference set of configurations for studying the lowest energy semi-flexible ($k_b > 0$) t-SHS polymer packings when there is a one-to-one mapping from the $N_{\rm micro}$ ground state polymer packings for $k_b = 0$ to the

---

[*]Electronic address: rshoy@usf.edu

$N_{\rm micro}$ lowest energy polymer packings with finite bending stiffness. More specifically, our approach assumes that the $N_{\rm micro}$ zero-k_b t-SHS packings lie within the basins[8] of the $N_{\rm micro}$ lowest-energy packings at finite k_b as shown in Fig. 1 (right). Increasing $k_b > 0$ deforms the energy landscape, raises the energies of the $N_{\rm micro}$ flexible polymer packings, and breaks their degeneracy. For $k_b < k_b^{\rm crit}$, the $N_{\rm micro}$ lowest energy semi-flexible polymer packings correspond to the $N_{\rm micro}$ ground-state flexible polymer packings. In contrast, for $k_b > k_b^{\rm crit}$ the energy landscape is sufficiently deformed that new low-energy packings (that do not belong to the set of $k_b = 0$ ground-state polymer packings) are among the N_{micro} lowest. For example, in Fig. 1 with $N_{\rm micro} = 8$, if the energy of polymer packing 9 drops below any of the energies of packings 1 through 8, $k_b > k_b^{\rm crit}$. Below, we will calculate the total energy (that includes bending and attractive contact energy terms) for the ground state t-SHS polymer packings as a function of k_b and determine $k_b^{\rm crit}$.

The pair potential for t-SHS polymers with spherical monomers of diameter D is[6, 9]:

$$U_{ss}(r) = \begin{cases} \infty & , \ r < D \\ -\epsilon & , \ r = D \\ 0 & , \ r > D \ , \ \text{noncovalent} \\ \infty & , \ r > D \ , \ \text{covalent}, \end{cases} \tag{1}$$

where r is the center-to-center separation between monomers and $-\epsilon$ is the contact energy. In Eq. 1, the term "covalent" ("noncovalent") refers to monomers that are (not) chemically adjacent and permanently connected. All $N_{\rm micro}$ distinguishable polymeric paths (microstates) through N-monomer, N_c-contact t-SHS packings are obtained via the complete enumeration procedure described in Ref. [6]. Values of $N_{\rm micro}$ for ground-state (maximal-N_c) t-SHS packings of $6 < N < 9$ monomers are given in Table I.

TABLE I: Number of microstates $N_{\rm micro}$ for maximally contacting t-SHS packings, where $N_{\rm micro}$ for $N > 6$ includes a factor of two associated with packings possessing chiral enantiomers.[10]

N	N_c	$N_{\rm micro}$
6	12	50
7	15	700
8	18	6429
9	21	122060

For numerical calculations, we employ a continuous version of $U_{ss}(r)$ with short-range attractive interactions and harmonic bond-length constraints illustrated in Fig. 2 (a),

$$U_c(r) = \begin{cases} -\epsilon + \dfrac{k_c}{2}\left(\dfrac{r}{D} - 1\right)^2 & , \ r < r_c \\ \\ 0 & , \ r \geq r_c, \end{cases} \tag{2}$$

where $r_c/D = \infty$ for covalently bonded monomers and $r_c = r_c^{nc} = D(1 + \sqrt{2\epsilon/k_c})$ for noncovalently bonded monomers. Note that $U_{ss}(r)$ is the $k_c \to \infty$ limit of U_c in Eq. 2. To model finite bending stiffness, we employ a harmonic bond-angle potential used in many previous computational studies of organic molecules, peptides, and proteins [11, 12]:

$$U_{\rm bend}^i = \frac{k_b}{2}\frac{(\theta^i - \theta^i_{eq})^2}{\pi^2}. \tag{3}$$

The bond angle θ^i between adjacent monomers (i, $i+1$, $i+2$) is defined as $\theta^i = \pi - {\rm acos}[(\vec{b}_i \cdot \vec{b}_{i+1})/|b_i b_{i+1}|]$, with $\vec{b}_i = \vec{r}_{i+1} - \vec{r}_i$. $U^i_{\rm bend}$ is minimized at the equilibrium bond angle $\theta^i = \theta^i_{eq}$, and k_b is expressed in units of ϵ.

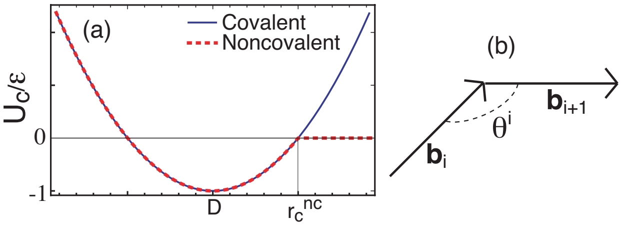

FIG. 2: Schematic of (a) the short-range attractive and harmonic bond-length potentials in Eq. 2 and (b) definition of the bond angle for the harmonic bond-angle potential in Eq. 3.

The total potential energy of an N-monomer chain is

$$U_{\rm chain} = \textstyle\sum_{i=1}^{N-1} \sum_{j>i}^{N} U_c(r_{ij}) + \sum_{i=1}^{N-2} U^i_{\rm bend}. \tag{4}$$

For $k_b = 0$ and the limit $k_c \to \infty$, configurations corresponding to local minima of $U_{\rm chain}$ are clearly identical to those obtained in studies of t-SHS packings with no bond-angle interactions, *i.e.* all N-monomer, N_c-contact microstates have $U_{\rm chain} = -N_c\epsilon$. Bond-angle interactions break this degeneracy; $U_{\rm chain}$ increases by different amounts for each microstate.

In the sticky hard sphere ($k_c \to \infty$) limit, to first order, increasing the bending stiffness does not change the structure of the polymer packings; in the limit $k_b/k_c \to 0$, the increase in energy $U_{\rm chain}(k_b) - U_{\rm chain}(k_b = 0)$ scales linearly with k_b. Each reference ($k_b = 0$) microstate possesses a set of $N-2$ "reference" bond angles $\{\theta_1^{ref},\ \theta_2^{ref},\ ...,\ \theta_{N-2}^{ref}\}$. Thus, the leading order (LO) prediction for the energy of the jth microstate is

$$U^j_{\rm chain,LO} = -N_c\epsilon + \frac{k_b}{2\pi^2} c_j(N, \theta_{eq}) \tag{5}$$

where

$$c_j(N, \theta_{eq}) \equiv \sum_{i=1}^{N-2} (\theta_i^{ref,j} - \theta_{eq})^2 \tag{6}$$

and we assume $\theta^i_{eq} = \theta_{eq}$ for all i. Since all c_j are available from the flexible t-SHS packings, LO predictions for the energy of polymer packings for arbitrary k_b

and θ_{eq} can be made using only information from the flexible reference polymer packings. Predictions for the minimum, maximum, and average energies of polymer packings (U_{min}, U_{max}, U_{avg}) from Eq. 5 for $N = 8$ and two physically relevant θ_{eq} are shown in Fig. 3. Alkanes and other polymers with tetrahedral bond-angle order have $\theta_{eq} \simeq \theta_{tet} = \mathrm{acos}(-1/3) = 109.47°$, while $\theta_{eq} = \pi$ corresponds to alkynes and other polymers with linear bond-angle order. The bond-angle energies are higher for $\theta_{eq} = \pi$ since the compact structure of small-N t-SHS packings allows few "straight trimers" (angles with $\theta^i = \pi$).

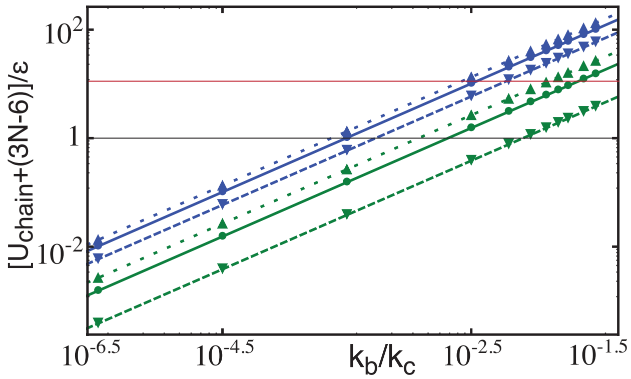

FIG. 3: Comparison of the leading-order expressions for the energy U_{chain} of $N = 8$ semiflexible polymer packings in Eq. 5 (dashed, U_{min}; solid, U_{avg}; dotted, U_{max}) to the numerical results for the energy of minimized t-SHS packings in the presence of bond-angle interactions (downward triangles, U_{min}; circles, U_{avg}; upward triangles, U_{max}) as a function of k_b/k_c. Results for $\theta_{eq} = \theta_{tet}$ and π are shown in green and blue, respectively. $U_{\mathrm{chain}}/\epsilon = -(N_c - 1)$ and $U_{\mathrm{chain}} = 0$ are respectively indicated by the black and red horizontal lines.

To validate the leading-order expressions for the energy of semiflexible polymer packings in Eq. 5, we employed energy minimization techniques (described in the Appendix) to relax the t-SHS configurations in the presence of bond-angle interactions. The leading-order expressions for the minimum U_{min}, average U_{avg}, and maximum U_{max} chain energies closely agree with the numerical results over a wide range of k_b/k_c as shown in Fig. 3. Both the numerical results and leading-order expressions for U_{chain} are nearly linear in k_b/k_c over the full range studied. We know that $k_b/k_c > k_b^{\mathrm{crit}}/k_c$ for $U_{\mathrm{chain}} > 0$ since freely-rotating chain conformations with no pair contacts and $\theta^i = \theta_{eq}$ for all bond angles have $U_{\mathrm{chain}} = 0$. Thus it is clear that the critical bending stiffness k_b^{crit} (above which the N_{micro} lowest energy semiflexible polymer packings are not the same as the N_{micro} ground-state t-SHS packings) is below $k_b^{\mathrm{crit}}/k_c \sim 10^{-1.5}$ where $U_{\mathrm{chain}} \gg -N_c\epsilon$.

For $N = 8$, we find that k_b exceeds k_b^{crit} at a relatively small value for the bending stiffness. Note that for $\theta_{eq} = \theta_{tet}$, $(U_{\mathrm{max}} + N_c\epsilon)/(U_{\mathrm{min}} + N_c\epsilon) \simeq 7$ because there is a large dispersion of bond angles in the t-SHS packings as shown in Fig. 4. The t-SHS packings possess a wide range of bond angles, leading to large $\Delta\theta$, and differently structured packings[6, 10, 13] and polymeric paths through these packings lead to large variations in $\langle\theta\rangle$. The variation in both $\langle\theta\rangle$ and $\Delta\theta$ increases rapidly with N.

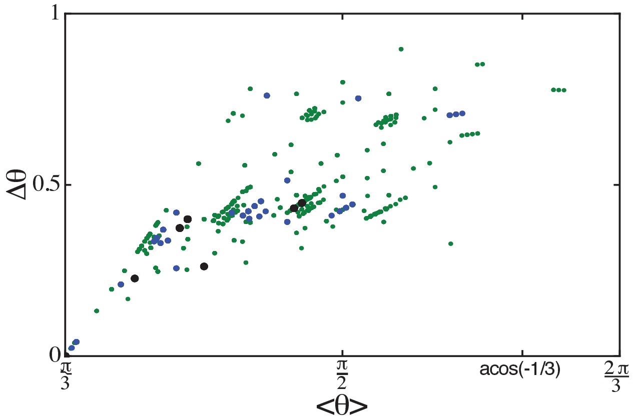

FIG. 4: Bond-angle dispersion for t-SHS polymer packings. Each data point represents the mean bond angle θ and the rms deviation $\Delta\theta$ for a single t-SHS polymer packing. Large black, medium blue, and small green circles represent data for $N = 6$. 7, and 8, respectively.

A more refined estimation of k_b^{crit} can be obtained as follows. The $N_{\mathrm{micro}}(N)$ flexible t-SHS packings all possess $N_c(N)$ pair contacts (Table I) and energy $-N_c(N)\epsilon$. Any polymer packing with fewer than $N_c(N)$ pair contacts must have $U_{\mathrm{chain}} \geq -(N_c - 1)\epsilon$ since the bending energy is strictly positive. Conversely, any t-SHS polymer packing with N_c pair contacts must correspond (in the sense of Fig. 1) to one of the $N_{\mathrm{micro}}(N)$ flexible t-SHS packings. Therefore $k_b^{\mathrm{crit}}(N, \theta_{eq})$ is set by the largest $c_j(N, \theta_{eq})$ (Eq. 6) for these packings and the condition that the reduced bending energy is less than unity, and thus

$$k_b^{\mathrm{crit}}(N, \theta_{eq}) \leq 2\pi^2/c_j^{max}(N, \theta_{eq}). \tag{7}$$

As shown in Fig. 5, k_b^{crit} decreases monotonically with increasing N for all $\theta_{eq} \geq \pi/3$, which stems from the increasing angular dispersion with N shown in Fig. 4. In addition, for increasing θ_{eq}, k_b^{crit} reaches a peak at θ_{max} that increases with N, and then decreases steadily for $\theta_{eq} > \theta_{\mathrm{max}}$. For the N considered here, the peak occurs at a rather small $\theta_{\mathrm{max}} \lesssim \pi/2$ because of the compactness of the flexible t-SHS reference polymer packings. Nonetheless, we expect the key result of decreasing k_b^{crit} with increasing N to continue for $N > 9$.

To check the analytic prediction of Eq. 7 for k_b^{crit}, we performed molecular dynamics simulations of semiflexible t-SHS chain collapse for $N = 8$. Monomers interact via the pair and bond-angle potentials in Eqs. 2 and 3, with $k_c = 3200\epsilon$ and a range of θ_{eq} and k_b. For each θ_{eq}, k_b, and k_c, systems of $N_{\mathrm{S}} = 1000$

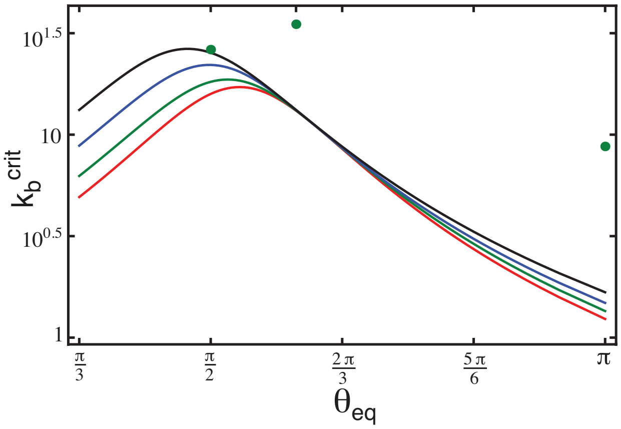

FIG. 5: Estimates of $k_b^{\mathrm{crit}}(N,\theta_{eq})$ from Eq. 7 for $N=6$ (black line), 7 (blue line), 8 (green line), and 9 (red line) and MD simulations of polymer collapse for $N=8$ (green circles).

independent self-avoiding random walk polymer configurations were slowly quenched from high temperature ($k_BT_i = 4\epsilon$) to $k_BT_f < 10^{-10}\epsilon$ using an isokinetic thermostat [14] and quench protocol $T = T_i \exp\left[-t/(10^3\tau)\right]$, where $\tau = \sqrt{mD^2/\epsilon}$ is the unit of time and m is the monomer mass. An overestimate of k_b^{crit} can be obtained by measuring the lowest k_b at which the minimum energy collapsed states obtained via MD have chain energies below U_{min}, which cannot correspond to any of the N_{micro} flexible t-SHS inherent structures.

A comparison of k_b^{crit} from Eq. 7 and estimates from the MD simulations are shown in Fig. 5 for several θ_{eq}. In all cases, the appearance of polymer packings with energies lower than U_{min} coincides with contact-breaking (*i.e.* the minimum energy semiflexible polymer packings from MD simulations possess fewer pair contacts than the flexible t-SHS inherent structures) and occurs for k_b^* that satisfy $[U_{\mathrm{max}}(k_b^*) + (3N-6)] \simeq (2-3)\epsilon$. Thus, energetically favorable rearrangements of t-SHS polymer packings due to finite bending stiffness require breaking two or three pair contacts.

We conclude that under our very strict condition that *all* of the N_{micro} lowest-energy zero-k_b t-SHS states must maintain a one-to-one correspondence to the N_{micro} lowest-energy states for finite k_b, the flexible t-SHS minimal energy packings are of limited utility as a basis for perturbative studies of polymers with finite bending stiffness. A less strict condition, *e.g.* requiring only a one-to-one correspondence for *ground* states, would allow extension of perturbative approaches to larger k_b. Nonetheless, our results suggest that even very small bending stiffness will dramatically alter the low-temperature equilibrium structure of t-SHS polymers from that of the $k_b = 0$ reference set, and that care should be taken in generalizing recent results obtained for flexible model polymers (*e.g.* Refs. [15–21]) to realistic polymers. In future studies, we will enumerate and characterize the structural and mechanical properties of minimal energy semiflexible polymer packings with $k_b > k_b^{crit}$ using Monte Carlo or molecular dynamics simulations with advanced sampling techniques.

Support from NSF Award No. DMR-1006537 is gratefully acknowledged. This work also benefited from the facilities and staff of the Yale University Faculty of Arts and Sciences High Performance Computing Center and NSF grant No. CNS-0821132 that partially funded acquisition of the computational facilities.

Appendix A: Structure solver for packings with finite k_c and k_b

We find the mechanically stable, minimal energy configuration $\{\vec{r}_{min}\}$ closest to each flexible packing $\{\vec{r}_{flex}\}$ by starting from configurations $\{\vec{r}_{pert}\}$ representing small random perturbations[22] away from $\{\vec{r}_{flex}\}$, and minimizing U_{chain}. Energy minimization is carried out using the "dog-leg" method [23], which is a combination of gradient descent and Newton's method [24]. Our numerical algorithm is schematically depicted in Figure 6.

For finite k_b, the first spatial derivatives of U_{chain} evaluated at $\{\vec{r}\} \neq \{\vec{r}_{min}\}$ are generally nonzero. We approach $\{\vec{r}\} = \{\vec{r}_{min}\}$ using gradient descent and a second-order expansion of $f(\{\vec{r}\}) \equiv U_{\mathrm{chain}}(\{\vec{r}\})$. This descent iteratively reduces f using

$$f_n^* = f_n - \alpha \nabla f_n, \tag{A1}$$

where f_n is the value of f at the nth minimization step, f_n^* is U_{chain} at the "knee" of the dog-leg [25], the optimal step length is [26]

$$\alpha = \frac{\nabla f (\nabla f)^T}{\nabla f H(f) (\nabla f)^T}, \tag{A2}$$

and $H(f_n)$ is the $3N \times 3N$ Hessian matrix of f_n. After the gradient descent step, we perform a least-squares Newton iteration on ∇f_n using step-length control [24] (Box 1):

$$f_{n+1} = f_n^* - \left(H^T(f_n^*) H(f_n^*)\right)^{-1} H^T(f_n^*) \nabla f_n^*. \tag{A3}$$

If the Frobenius norm $||\nabla f_{n+1}||_2$ of ∇f_{n+1} decreases (*i.e.* $||\nabla f_{n+1}||_2 < ||\nabla f_n^*||_2$), we check whether$f_{n+1} < f_n^*$. If $f_{n+1} > f_n^*$, we set $f_{n+1} = f_n^*$; if $f_n^* \geq f_n$, the gradient descent has failed and we set $f_n^* = f_n$ in Eq. A3. We then check whether $||\nabla f_{n+1}||_2 \leq ||\nabla f_n^*||_2$; if so, Equations A1-A3 represent one complete minimization step taking $f_n \to f_{n+1}$ (Boxes 1-2). Otherwise, if $||\nabla f_{n+1}||_2 > ||\nabla f_n^*||_2$ the minimization algorithm has failed (Box 3); however, this occurs only for k_b much larger than those considered here.

The minimization procedure reduces the first spatial derivatives of U_{chain} to zero. When this condition is satisfied ($\nabla f = 0$), we check whether $\{\vec{r}\}$ represents a mechanically stable solution, *i.e.* whether all $3N-6$ nontrivial eigenvalues of H are positive (Box 4). Saddle-point solutions are avoided (when encountered) by perturbing

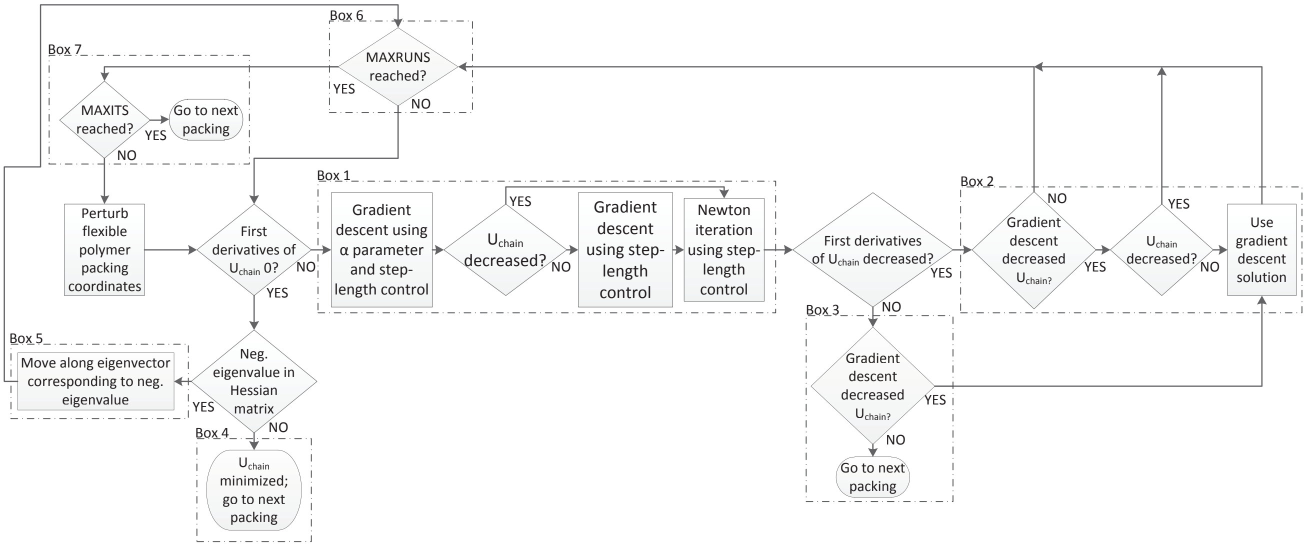
Box 7
MAXITS reached?
YES
Go to next packing
NO
Box 6
MAXRUNS reached?
YES
NO
Perturb flexible polymer packing coordinates
First derivatives of U$_{chain}$ 0?
NO
YES
Box 1
Gradient descent using α parameter and step-length control
YES
U$_{chain}$ decreased?
NO
Gradient descent using step-length control
Newton iteration using step-length control
First derivatives of U$_{chain}$ decreased?
YES
NO
Box 2
NO
Gradient descent decreased U$_{chain?}$
YES
YES
U$_{chain}$ decreased?
NO
Use gradient descent solution
Box 5
Move along eigenvector corresponding to neg. eigenvalue
YES
Neg. eigenvalue in Hessian matrix
NO
Box 4
U$_{chain}$ minimized; go to next packing
Box 3
Gradient descent decreased U$_{chain?}$
YES
NO
Go to next packing

FIG. 6: Flowchart depicting the algorithm used to find the mechanically-stable, minimum-energy configuration $\{\vec{r}_{min}\}$ closest to each flexible packing configuration $\{\vec{r}_{flex}\}$.

coordinates along a negative eigenvector of the Hessian matrix (Box 5).

Finally, should the solver reach the maximum number of iterations for a particular $\{\vec{r}_{pert}\}$ (MAXRUNS; Box 6) we attempt to minimize a different $\{\vec{r}_{pert}\}$, for up to MAXITS different $\{\vec{r}_{pert}\}$ (Box 7). We found that MAXITS = 1000 different $\{\vec{r}_{pert}\}$ with a maximum of 50 iterations per $\{\vec{r}_{pert}\}$ to be sufficient to minimize the energy or determine that no minimum that preserves the adjacency matrix exists for the $N \leq 9$ polymer packings considered here.

[1] P. J. Flory, C. A. J. Hoeve, and A. Ciferri, J. Poly. Sci. **34**, 337 (1959).

[2] G. N. Ramachandran and V. Sasisekharan, Adv. Prot. Chem. **23**, 284 (1968).

[3] F. M. Richards, Ann. Rev. Biophys. Bioeng. **6**, 151 (1977).

[4] S. Sacanna, W. T. M. Irvine, P. M. Chaikin, and D. J. Pine, Nature **464**, 575 (2010).

[5] M. J. Solomon, Nature **464**, 496 (2010).

[6] R. S. Hoy and C. S. O'Hern, Phys. Rev. Lett. **105**, 068001 (2010).

[7] S. Schnabel, M. Bachmann, and W. Janke, J. Chem. Phys. **131**, 124904 (2009).

[8] F. H. Stillinger, Science **267**, 1935 (1995).

[9] S. B. Yuste and A. Santos, Phys. Rev. E **48** (1993).

[10] N. Arkus, V. N. Manoharan, and M. P. Brenner, Phys. Rev. Lett. **103**, 118303 (2009).

[11] P. C. Cross and J. H. Van Vleck, J. Chem. Phys. **1**, 350 (1933).

[12] S. Toxvaerd, J. Chem. Phys. **107**, 5197 (1997).

[13] R. S. Hoy, J. Harwayne-Gidansky, and C. S. O'Hern, Phys. Rev. E **85**, 051403 (2012).

[14] D. Brown and J. H. R. Clarke, Mol. Phys. p. 1243 (1984).

[15] M. P. Taylor, J. Chem. Phys. **118**, 883 (2003).

[16] M. P. Taylor, W. Paul, and K. Binder, J. Chem. Phys. **131**, 114907 (2009).

[17] M. P. Taylor, W. Paul, and K. Binder, Phys. Rev. E **79** (2009).

[18] D. T. Seaton, T. Wüst, and D. P. Landau, Phys. Rev. E **81**, 011802 (2010).

[19] G. T. Evans, J. Chem. Phys. **134**, 044902 (2011).

[20] R. S. Hoy and C. S. O'Hern, Soft Matter **8**, 1215 (2012).

[21] S. Růžička, D. Quigley, and M. P. Allen, Phys. Chem. Chem. Phys. **14**, 6044 (2012).

[22] Each monomer position is perturbed by a maximum amplitude $|\delta\vec{r}|_{max} = 0.2$, which was chosen to optimize the efficiency of the structure solver while satisfying the requirement $|\delta\vec{r}|_{max} < (\sqrt{2} - 1)/2$ for preserving chain topology.

[23] J. E. Dennis, Jr. and R. B. Schnabel, *Numerical Methods for Unconstrained Optimization and Nonlinear Equations* (Classics in Applied Mathematics, v. 16: Soc. for Industrial & Applied Math., 1996).

[24] W. Press, S. A. Teukolsky, W. T. Vetterling, and B. P. Flannery, *Numerical Recipes: The Art of Scientific Computing (3rd ed.)* (Cambridge University Press, 2007).

[25] In the event that $U_{\rm chain}$ does not decrease, we attempt gradient descent with step-length control without the α parameter, *i.e.* $f_n^* = f_n - \nabla f_n$.

[26] M. Powell. A Hybrid Method for Nonlinear Equations. In P. Rabinowitz, editor, Numerical Methods for Nonlinear Algebraic Equations, pages 87144. Gordon and Breach Science, London, 1970.